Soft Matter

PAPER

View Article Online
View Journal | View Issue

Cite this: *Soft Matter*, 2016, **12**, 8167

Passive microrheology in the effective time domain: analyzing time dependent colloidal dispersions†

Bhavna M. Vyas,[ab] Ashish V. Orpe,*[a] Manish Kaushal‡[b] and Yogesh M. Joshi*[b]

Received 6th April 2016,
Accepted 30th August 2016

DOI: 10.1039/c6sm00829a

www.rsc.org/softmatter

We studied the aging dynamics of an aqueous suspension of LAPONITE®, a model time dependent soft glassy material, using a passive microrheology technique. This system is known to undergo physical aging during which its microstructure evolves progressively to explore lower free energy states. Optical microscopy is used to monitor the motion of micron-sized tracer probes embedded in a sample kept between two glass plates. The mean square displacements (MSD) obtained from the motion of the tracer particles show a systematic change from a purely diffusive behavior at short aging times to a subdiffusive behavior as the material ages. Interestingly, the MSDs at all the aging times as well as different LAPONITE® concentrations superpose remarkably to show a time–aging time master curve when the system is transformed from the real time domain to the effective time domain, which is obtained by rescaling the material clock to account for the age dependent relaxation time. The transformation of the master curve from the effective time domain to the real time domain leads to the prediction of the MSD in real time over a span of 5 decades when the measured data at individual aging times are only over 2 decades. Since the MSD obtained from microrheology is proportional to the creep compliance of a material, by using the Boltzmann superposition principle along with the convolution relation in the effective time domain, we predict the stress relaxation behavior of the system in real time. This work shows that the effective time approach applied to microrheology facilitates the prediction of long time creep and relaxation dynamics of a time dependent soft material by carrying out short time experiments at different aging times.

I. Introduction

Time dependent soft materials are thermodynamically out of equilibrium. Their microstructure evolves as a function of time by undergoing reorganization or physical aging to take the system to a progressively lower free energy state.[1] There are many industrially important materials that fall in this category such as highly concentrated suspensions and emulsions, industrial (including agrochemical and pharmaceutical) pastes, colloidal gels, various types of paste-like food products, *etc.* The physical aging that takes place in these materials can sometimes be extremely sluggish and continues over very large timescales. This may affect the behavior of a product stored over long durations. Furthermore, in these materials structural build-up takes place over different length scales. Consequently, their rheological behavior is also dependent on length scales, whose knowledge is important when such materials are used in miniature systems such as microfluidic devices, micro-reactors, *etc.* Over the past two decades, microrheological techniques have been developed, wherein by monitoring/controlling the motion of submicron size tracer particles in soft materials, rheological properties at very small length scales can be obtained.[2–7] In this work, we studied an aqueous suspension of LAPONITE®, a model time dependent soft material, and obtain its rheological behavior over microscopic length scales using passive microrheology. More importantly, we propose an effective time methodology in conjunction with microrheology to obtain very long time rheological behavior by carrying out a few tests at short times.

Microstructural evolution to attain progressively lower free energy states as a function of time is a very natural response of materials that are thermal in nature and have been kinetically constrained from achieving the thermodynamic equilibrium state. Soft materials that fall in this category have been termed as soft glassy materials in the literature.[8] The mesoscopic

[a] *Chemical Engineering Division, National Chemical Laboratory, Pune 411 008, India. E-mail: av.orpe@ncl.res.in*
[b] *Department of Chemical Engineering, Indian Institute of Technology Kanpur, Kanpur 208016, India. E-mail: joshi@iitk.ac.in*

† Electronic supplementary information (ESI) available. See DOI: 10.1039/c6sm00829a

‡ Present address: Laboratoire de Physique des Solides, CNRS, Univ. Paris-Sud, Université Paris-Saclay, 91405 Orsay Cedex, France.

elements that constitute these materials are structurally arrested in energy wells formed due to their interactions with neighboring elements. Since the well depths that arrest the mesoscopic elements are significantly larger than the thermal energy, a material as a whole is unable to achieve the thermodynamic equilibrium state.[9] These elements undergo microscopic dynamics during structural rearrangements and on an average sink in their own well or a new well with a deeper depth as a function of time. By virtue of the distribution of energy well depths there exists a distribution of relaxation times. As various elements age with time, the distribution shifts to slower relaxation modes. Owing to time dependency, these materials do not obey time translational invariance, and consequently the fundamental principles of linear viscoelasticity are not applicable to them.[1] Joshi and coworkers,[10–12] through a series of papers, proposed that the concept of time translational invariance can be applied to these materials by transforming their behavior from the real time domain to an effective time domain. In an effective time domain, time is normalized by the mean relaxation time so that the relaxation dynamics become invariant of aging time. The work by Joshi and coworkers did not simply validate the Boltzmann superposition principle and time temperature superposition principle for soft glassy materials, but also validated the convolution relation that relates two response functions, namely modulus and compliance, with each other.[11,12] Very importantly, this methodology allows the use of either the short time creep or stress relaxation behavior of a time dependent material to obtain a long time prediction of the other. However, in order to apply this methodology, aging should affect only the mean value of the relaxation times and not the shape of their distribution.[13] While the above work by Joshi and coworkers has been carried out using bulk rheology measurements, it is quite pertinent to assess whether similar analysis can be extended to measurements carried out at a microscopic level. The need for analysis at a microscopic level is specifically important in spatially inhomogeneous systems wherein the bulk rheology can only provide average measurements, thus, precluding rich behavior that may occur at a local level, and which may not match the bulk measurements.

One of the well-known techniques to carry out microscopic measurements in a sample is particle tracking microrheology.[3] This involves tracking the motion of micron-sized tracer particles suspended in a sample, which are driven by inherent thermal fluctuations (of the order of k_BT).[14–17] Since the motion is governed by the state of a system and not driven by any active external force, this technique is also termed as passive microrheology. It should be noted that the suspension system needs to be soft enough to allow the motion of the tracer particles only on the basis of k_BT for a system. The motion of the tracer particles can be detected using microscopy, dynamic light scattering (DLS) or diffusive wave spectroscopy (DWS). The detected centers of the tracer particles, using standard particle tracking algorithms,[18] are used to obtain individual particle displacements, and the ensemble average over all the tracer particles provides the mean square displacement $\langle r^2(t_{lag})\rangle$ as a function of lag time (t_{lag}), which is defined as the time elapsed since mean square displacement measurements have started. Using the Langevin equation for diffusing micron sized particles with radius a having a spherical shape, the unilateral Laplace transform [for any arbitrary function: $\tilde{f}(s) \equiv \mathcal{L}\{f(t)\} \equiv \int_0^\infty e^{-st} f(t)dt$, where s is the Laplace frequency] of the complex shear modulus [$\tilde{G}(s)$] can be related to the Laplace transform of $\langle r^2(t)\rangle$ as:[3,19,20]

$$\tilde{G}(s) = \frac{s}{6\pi a}\left[\frac{6k_BT}{s^2\langle\tilde{r}^2(s)\rangle} - ms\right] \approx \frac{k_BT}{\pi a s\langle\tilde{r}^2(s)\rangle}. \quad (1)$$

The Laplace transform of the stress relaxation modulus [$\tilde{G}_r(s)$] is related to $\tilde{G}(s)$ as: $G(s) = s\tilde{G}_r(s)$,[3,19,20] while the creep compliance ($J(t)$) is related to the stress relaxation modulus as:[21]

$$t = \int_0^t J(t-t')G_r(t')dt' \quad \text{or}$$
$$\mathcal{L}\{J(t)\}\mathcal{L}\{G_r(t)\} = \tilde{J}(s)\tilde{G}_r(s) = 1/s^2. \quad (2)$$

Using eqn (1) and (2), and taking the inverse Laplace transform, $J(t)$ can be related to $\langle r^2(t)\rangle$ as:[3,19,20]

$$J(t) = \frac{\pi a}{k_BT}\langle r^2(t)\rangle. \quad (3)$$

The Stokes–Einstein equation, which is valid for Newtonian fluids, has been generalized using this method to analyze viscoelastic fluids with frequency dependent linear viscoelastic moduli. The underlying assumption is that the inertial effects on the motion of the tracer particles are negligibly small. It is to be noted that if a size of a tracer particle is much larger than the characteristic structural length scale in a system, then the measurements resemble the bulk rheology measurements. However, if the size of a tracer particle is comparable to the structural length scale, then the measured rheology at the local level may or may not match the bulk rheological measurements, particularly for highly inhomogeneous systems.[17] Using passive microrheology, it is also possible to explore individual tracer particle motion, and not necessarily obtain ensemble averages, to get an insight into the local environment in the vicinity of the tracer particles.[22] In certain cases, for instance, the probes in active biological samples exhibit a complex behavior comprising caging and diffusive–convective motions spread over very long time scales, which are difficult to ascertain through experiments. To address this issue, Weihs *et al.*[23] introduced a time-domain analytical method, which is capable of using the MSD data from the probe trajectories over a shorter time and then generates the probe behavior over a much wider time domain exhibiting the inherent complexities in such complex systems. More details on microrheological approaches can be found in the available literature.[2,3,7]

Various paste-like systems such as Carbopol suspensions,[24] gellan gum,[25] peptide dispersions,[26] hectorite clay dispersions,[27] *etc.* have been studied using microrheology techniques. However, in this paper, we concentrate only on the microrheology studies of the time dependent materials that are relevant to the present work. Houghton *et al.*[27] used passive microrheology to study the gelation of aging hectorite clay suspensions. The results showed increasing inhomogeneity in the samples with time as

exhibited by the anisotropy in the curves for the mean square displacements in different spatial directions. A precise gel point was obtained by Larsen and Furst[28] for a time dependent physical (peptide) gel and a concentration dependent chemical (polyacrylamide) gel. The mean square displacements of the probe particles were separated into two master curves using suitable shift factors: one before the gel point and one after the gel point. The shift factors for both, pre- and post-gel point regimes, exhibited divergence at a unique time (for a physical gel) and concentration (for a chemical gel) which represented the critical state. Interestingly, at the gel point, the critical relaxation exponent and the dynamic scaling exponents showed remarkable agreement with the predictions from the theories for fractal polymers. The kinetics of peptide self-assembly was studied using microrheology by Savin and Doyle.[26] An increase in the self-assembly of the peptide led to a subdiffusive behavior exhibited by the probe mean square displacements, suggestive of a gel formation. The gel point was determined by the congruency of the frequency dependence of the viscous and elastic moduli[29] as calculated from the mean square displacements. It was also observed that the pH of the solution has a profound effect (almost hundred-fold) on the gelation time, even at a very low concentration of peptide. The mechanism of gelation, though, was found to be independent of pH.

Quite recently, a few groups have used the microrheology technique to study the aging behavior for LAPONITE® suspensions, which is a subject matter of this work. Abou and Gallet[30] carried out an experimental study to check the validity of the fluctuation–dissipation theorem for an aging LAPONITE® suspension. Their measurements revealed a non-monotonic variation of the effective temperature with increasing aging times, with the maximum corresponding to about twice the batch temperature. The observed behavior was attributed to the possible evolution of the relaxation time distribution expected in a system with evolving heterogeneity. However, subsequent work by Jabbari-Farouji[31] showed that the effective temperature remains constant and does not differ from the bath temperature over a much wider range of aging times, thus, implying no violation of the fluctuation–dissipation for such non-equilibrium systems. The reasons for the qualitative differences between these and the measurements made by About and Gallet[30] are, however, not quite clear, except perhaps the use of different concentrations of LAPONITE® in each study. The measurements made by Jabbari-Farouji[31] also revealed that the overall viscoelasticity in the system arises from two contributions, *viz.* the strong frequency dependent response at high frequencies and a more elastic response (weakly dependent on frequency) during the aging.

Oppong *et al.*[32] studied the gelation of 1 weight% LAPONITE® suspension using a microrheology technique with 0.5 micron radius microspheres as the probe particles. The magnitude of the viscous and elastic moduli obtained from the mean square displacements of the probe particles increased with the aging time. At short aging times, the viscous modulus was found to be larger than the elastic modulus indicating a viscous behavior while at longer times the trend was reversed, suggestive of a solid-like structure. In agreement with the theory of Winter–Chambon,[29] the elastic and viscous moduli showed identical dependence on frequency at the gel point. Qualitatively similar results were obtained from the measurements of bulk rheology, although the gel point was found to occur much earlier than that obtained from microscopic measurements. This difference in the gel point obtained from two measurements was attributed to the difference in the length scale at which the rheology is probed. While the bulk rheology being probed at a larger length scale considers a material to be a critical gel, the probe particles in the same sample are relatively free to move due to several vacant regions, thus perceiving the same sample as a fluid on a microscopic scale. With more aging time, the aggregates continue to grow and eventually the fluid regions are diminished completely, which leads to freezing of the probe particles, and hence perceiving the sample as a gel at a later time on a microscopic scale. The gel time, thus, shows an inverse relationship with the length scale being probed. This aspect was further explored by Rich *et al.*,[33] who found that the gel time increases by an order of magnitude for nearly one-fourth reduction in the probe particle size. The observed behavior suggests that the heterogeneity in the system changes with aging time, *i.e.* the sample microstructure evolves with aging time causing a continual increase in the solid-like behavior. The detailed microstructure as studied by the authors in terms of the heterogeneity ratio and correlation between successive displacements provides evidences of microstructural confinement. For different LAPONITE® concentrations, the authors identified a probe size–concentration superposition for the gelation time data. The scaling exponents were found to be dependent on probe sizes and LAPONITE® concentration.

We believe that since time dependent materials do not obey time translational invariance, microrheological analysis poses difficulties. Particularly, eqn (1)–(3) are applicable only for a small enough lag time for which the time dependency can be neglected and therefore time translational invariance can be assumed to be valid. However, the consideration of very small lag times does not allow generation of substantial amount of data. This problem can be partly addressed by extending the effective time domain framework, which has been developed for bulk rheological analysis, to microrheology. In this work, we develop such framework for microrheological analysis by considering an example of aging (time dependent) aqueous suspension of LAPONITE®.

II. Material, sample preparation and experimental protocol

LAPONITE® is an inorganic synthetic clay with primary particles having a disk-like shape with diameter 25 nm and thickness 0.92 nm. In an aqueous medium with pH around 10, its edge is positively charged while the faces are negatively charged. Soon after the incorporation of LAPONITE® in water beyond 1 weight% under vigorous stirring, it forms a clear suspension, whose viscoelastic properties show spectacular evolution as a function of time. Eventually it leads to the formation of a soft solid that

sustains its weight against gravity. The microstructure of the suspension that is responsible for the time dependent evolution of its viscoelastic properties (physical aging) is proposed to be due to a combination of attractive as well as repulsive interactions among the particles.[34,35]

In a typical sample preparation protocol, dry LAPONITE® XLG powder (dried over 4 hours at 120 °C) is gradually added to deionized, distilled water having pH 10 (using NaOH) containing 4 mM NaCl to obtain a suspension. The resulting mixture is stirred vigorously for about 30 min using a turrax drive and then passed through a microfilter (0.45 μm mesh, PRAMA® Nylon – non-sterile) to break the aggregates. This represents the initial state of a suspension (t_w = 0) for every experiment performed. Following filtration, fluorescent polystyrene microparticles of 1 μm diameter and density 1.05 g cc^{-1} are randomly dispersed in the suspension *via* rapid (∼15 s) vortex mixing. The fluorescent particle concentration is just enough to visualize sufficient number of particles for better statistics. In this work, we prepare suspensions using three LAPONITE® concentrations, 1.8, 2 and 2.2 weight%, all containing 4 mM NaCl. Hereafter, we shall represent the suspensions only by the LAPONITE® concentration without mentioning the salt concentration.

For the bulk rheology experiments, a freshly prepared filtered LAPONITE® suspension is introduced in the Couette cell (a concentric cylinder geometry with an outer diameter of 18.08 mm and a gap of 1 mm) of an Anton Paar MCR 301 rheometer. A suspension is then subjected to successive frequency sweeps (of 0.628–10 rad s^{-1}) with a stress magnitude of 0.1 Pa. A thin layer of low viscosity silicon oil is applied on the free surface of a sample in order to prevent evaporation of water over the duration of the experiment.

For the microrheological experiments a freshly prepared filtered sample is placed in a glass slide having a small rectangular cavity (volume ∼ 0.045 cm^3) in the center, which is then sealed using a cover slip. The fluorescent microspheres in the cavity are imaged using an inverted fluorescence microscope (Carl Zeiss) equipped with a 40× objective to give a spatial resolution of 0.323 microns per pixel. The images are taken in the center of the cavity to prevent any end wall effects. The fluorescent particle concentration used ensures about 50 particles in the microscope's field of view. A sequence of images is acquired up to a duration of 60 s lag time, at varying aging times (t_w) from the same sample position, using a camera operated at 20 frames per second. The duration of image acquisition is very small to expect any significant changes in the suspension properties during the course of measurements. All the measurements were made at 25 °C. Each such experiment was repeated three times using a fresh sample of LAPONITE® and the data shown in the figures represent the average over the three experiments.

The image sequence at all the aging times (from each experiment) is analyzed using standard particle tracking algorithms[18] to obtain the microsphere particle trajectories from the identified particle centers in each image. The particle trajectories are further analyzed to obtain the mean square displacements defined as $\langle r^2(\tau')\rangle = \langle |x(t+\tau') - x(t)|^2 + |y(t+\tau') - y(t)|^2\rangle$, where t is the arbitrary time, τ' is the lag time between two particle positions on a trajectory and (x,y) represents the two-dimensional spatial field for particle displacements. The angle brackets $\langle\cdot\rangle$ indicate the mean over all the particles in an image window. Each such mean value, for a given lag time, is further averaged over three experiments and the figures represent these average values.

III. Results and discussion

We first discuss the linear viscoelastic behavior over macroscopic (bulk) length-scales, which is obtained by subjecting a time dependent suspension sample to successive cyclic frequency sweeps in a rheometer. In Fig. 1(a) we plot the time evolution of G' and G'' of a freshly prepared 2 weight% system for ω = 10 rad s^{-1}. It can be seen that in the limit of small times G', which is smaller than G'', evolves at a faster rate and eventually crosses G''. Beyond the crossover point G' continues to increase while G'' shows a plateau. In Fig. 1(b) we plot G' and G'' as a function of ω for t_w = 1800 s, which shows G' to be a weak function of ω and to be greater than G'' throughout over the explored frequency window. The observed rheological behavior very clearly indicates the soft glassy (pasty) nature of the studied LAPONITE® suspension.

The dynamics over microscopic length-scales are obtained by the mean square displacement of the tracer particles.

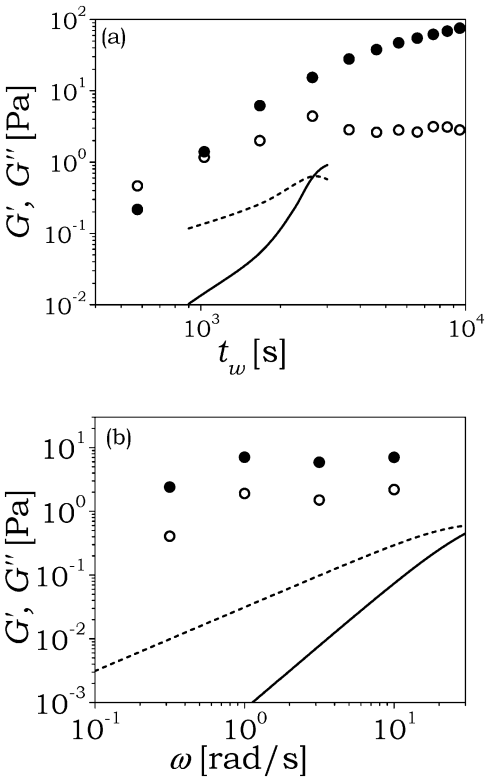

Fig. 1 The elastic (G', filled symbols and full line) and viscous (G'', open symbols and dashed line) moduli are plotted as a function of (a) t_w for ω = 10 rad s^{-1} and (b) ω for t_w = 1800 s. The symbols represent the experimental data while the lines represent the prediction from the microrheology experiments.

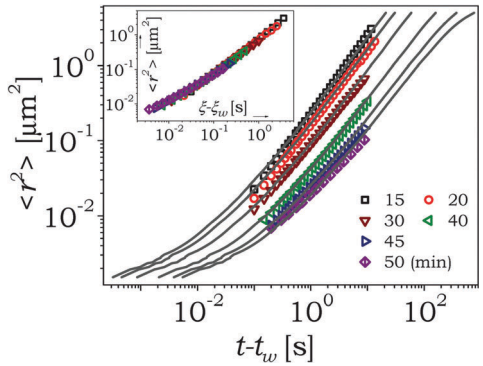

Fig. 2 MSD($\langle (r(t-t_w))^2 \rangle = (k_BT/\pi a)J(t-t_w)$) is plotted as a function of $t - t_w$ for different t_w for 2 weight% suspension. The symbols represent the experimental data while the solid lines represent prediction using eqn (10). The inset shows the transformed data (shown in main figure) in the effective time domain using eqn (8) for $\alpha = 0.077 \pm 0.0013$, which demonstrates time–aging time superposition, and thus validates the effective time-translational invariance.

The variation of the ensemble mean square displacements $\langle r^2(t-t_w)\rangle$ with experimental time $(t - t_w)$ is shown for several aging (or aggregation) times t_w in Fig. 2. For all the aging times, $\langle r^2(t-t_w)\rangle$ increases with $t - t_w$. However, the increase in $\langle r^2(t-t_w)\rangle$ gets slower with an increase in the aging time, which is suggestive of a progressive enhancement in the constrained dynamics, which arises due to restricted motion of the tracer particles indicating a cage-like surrounding caused by the microstructure build-up in the system.

The distributions of the displacements of individual particles are shown in Fig. 3 for the aging times reported in Fig. 2. The displacements are obtained over a duration of 1 second for each aging time. The motion of particles is isotropic and hence the distributions are shown only for the displacements in one spatial (x) direction. For t_w = 15 min or earlier (not shown), the distribution is Gaussian in nature as indicated by the solid line. The Gaussian distribution essentially represents a homogeneous system, devoid of any microstructure, allowing tracer particles to exhibit a random (purely diffusive) motion. The distribution progressively deviates from a Gaussian as t_w increases. This deviation represents a gradual enhancement in subdiffusive dynamics caused by microstructure evolution, leading to spatially variant tracer particle motion. The spatial variation arises due to particles located in different regions sampling different local behavior, which is dependent on the specific microstructure in the system. For very large values of t_w, the distribution is extremely narrow, which suggests that most of the tracer particles are in an immobilized state or are localized for the entire experimental time duration and the system is in a structurally arrested state.

The deviation of the displacement distribution from the Gaussian shape can be quantified in terms of the non-Gaussian parameter, N, defined as:[24]

$$N = \frac{\langle \Delta x^4 \rangle}{3\langle \Delta x^2 \rangle} - 1 \quad (4)$$

where, $\Delta x = |x(t+\tau) - x(\tau)|$, t is arbitrary time and τ is the lag time between the two particle positions in a trajectory. The closer the value of N is to zero, the closer a distribution represents a Gaussian that corresponds to a diffusive behavior. The variation of N with lag time $(t - t_w)$ obtained at different aging times (t_w) is shown in Fig. 4. It can be seen that the value of N increases with increasing t_w. Further, the value of N decreases sharply with $t - t_w$ at early aging times ($t_w < 30$ min), suggestive of an approach towards diffusive behavior accompanied by a Gaussian distribution seen in Fig. 3. For the longer aging times ($t_w > 40$ min), the decrease in the value of N becomes weak with $t - t_w$, suggesting that a diffusive behavior cannot be achieved for such aged systems over the range of explored lag times. This behavior matches well with that reported in the literature.[24]

The behavior observed in Fig. 2 and 3 is corroborated by the sample trajectories obtained at different aging times shown in Fig. 5. Every trajectory is recorded over an experimental time

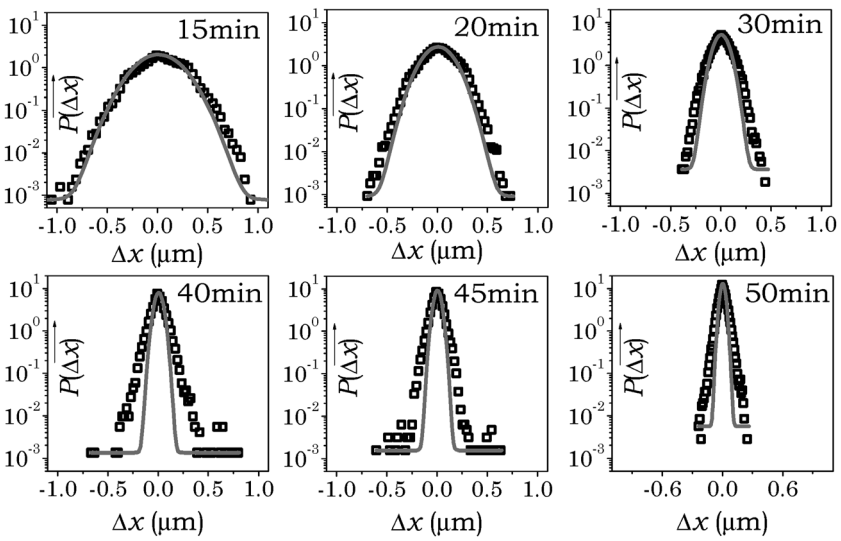

Fig. 3 Probability distribution curves of displacements for different t_w for a 2 weight% suspension. The solid lines represent the Gaussian fit to the experimental data shown in symbols. The data are shown only for x-direction displacements as the y-direction displacements exhibit similar behavior.

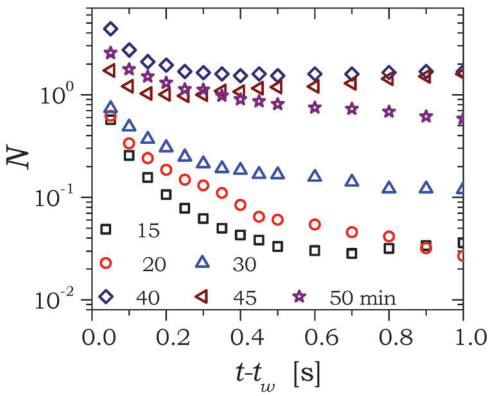

Fig. 4 Non-Gaussian parameter N plotted as a function of lag time ($t - t_w$) for different aging times.

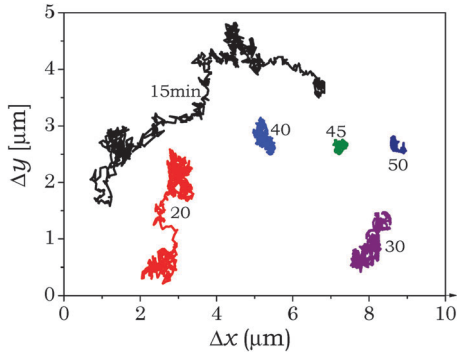

Fig. 5 Sample trajectories recorded over 60 s for different aging times (t_w = 15, 20, 30, 40, 45, and 50 min) for 2 weight% suspension.

of 60 seconds. As expected, the trajectory at t_w = 15 minutes shows significant particle movement, exploring a much larger space, in a homogeneous (liquid-like) state of the system. At subsequent aging times, with progressive evolution of the microstructure in the system, the movement of the tracer particle is significantly reduced, which is almost of the order of particle size for t_w = 50 minutes and even smaller at further aging times (not shown).

The above discussion provides reasonable signatures of an evolving microstructure within the static LAPONITE® suspension system with increasing aging times, which are in agreement with the previous microrheology studies on time evolving systems.[28,32,33,36] The data from the experiments, though conducted separately at each t_w, provide a clear picture of a continual, monotonic evolution of the suspension microstructure over time leading to its eventual structural arrest. Fig. 2 also depicts an important difference between the behavior of the MSD for materials that are at thermodynamic equilibrium and those materials that undergo time evolution. In the former, the MSD is only a function of lag time ($t - t_w$): $\langle r^2 \rangle = \langle r^2(t - t_w) \rangle$, while, in the latter, the MSD is also dependent on the time at which the system is explored (t_w, in the present case it is the same as aging time) in addition to that of lag time:

$$\langle r^2 \rangle = \langle r^2(t - t_w, t_w) \rangle \quad (5)$$

This behavior confirms the failure of time translational invariance and is attributed to the increase in the solid-like characteristics of the system with the increase in t_w. As shown in Fig. 2, the range of lag times ($t - t_w$) used to obtain MSDs for every individual t_w is very small compared to t_w. As a result, over a lag time ($t - t_w$), the change in the relaxation time (τ) is so small compared to its actual value that the relaxation time can be considered to be a constant, and the overall time dependency of the structural evolution is, thus, ignored. Consequently, eqn (1)–(3) can be applied to the MSD data at each t_w individually. The behavior shown in Fig. 2 therefore corroborates well with the creep compliance behavior observed for a variety of physically aging materials[10,37–40] that show $J = J(t - t_w, t_w)$, confirming the relationship expressed by eqn (3). It should be noted that the usage of MSD data over a limited time range, as is the case in the present work, is known for time-dependent complex fluids studied previously.[23]

Through a series of papers, Joshi and coworkers proposed the effective time domain approach[10–12,41] in order to accommodate the dependence of rheological response functions (in this case creep compliance through MSD) on t_w. On one hand, such an approach validates effective time translational invariance and allows the representation of the Boltzmann superposition principle in the conventional form, but in the effective time domain.[11,12] On the other hand, such an approach allows the prediction of very long time rheological behavior from short time experiments.[10] In the subsequent paragraphs, we try and extend the effective time domain approach to the microrheology of an aging LAPONITE® suspension, an example of a time dependent material.

It is well known that the viscoelastic response of a material depends primarily on the spectrum of relaxation time scales. In glassy materials, including that of soft glassy materials, it is usually observed that during physical aging, all the relaxation modes evolve with time in such a way that the shape of relaxation time spectrum is preserved. Under such conditions, based on the work of Hopkins[42] and Struik,[43] Joshi and coworkers proposed the effective time domain (ξ) as:[10–12,42,43]

$$\xi(t) = \bar{\tau} \int_0^t dt'/\tau(t'), \quad (6)$$

where, $\tau(t')$ is average relaxation time. It is proposed that for any arbitrary time, the dependence of relaxation time on time [$\tau = \tau(t)$] in transforming the material frame from the real time domain to the effective time domain given by eqn (6) leads to the cessation of time dependency such that the material assumes a constant relaxation time ($\bar{\tau}$).

According to eqn (6), the dependence of relaxation time on the aging time is required to transform aging time dependent MSD data to the effective time domain. Now, the available literature states that the relaxation time of the aqueous LAPONITE® suspension, immediately following its preparation, shows exponential dependence on aging time given by:[10,44,45]

$$\tau(t') = \tau_0 \exp(\alpha t'), \quad (7)$$

where, τ_0 and α are the fitting parameters. The incorporation of eqn (7) into eqn (6) and setting $\bar{\tau} = \tau_0$ lead to:

$$\xi - \xi_w = \frac{\exp(-\alpha t_w) - \exp(-\alpha t)}{\alpha}. \quad (8)$$

In the inset of Fig. 2, we show the variation of MSD with $\xi - \xi_w$. The MSD data at different t_w shows excellent superposition using $\alpha = 0.077 \pm 0.0013$. The existence of such time–aging time superposition validates effective time translational invariance on one hand and assumed relaxation time dependence shown by eqn (7) on the other hand. It is important to note that the relaxation time dependence that leads to superposition in the effective time domain is known to match the relaxation time dependence obtained from an independent measurement of relaxation time.[12] An identical qualitative behavior is also observed for two other concentrations of LAPONITE® (1.8 and 2.2 weight%) studied. The behavior of $\langle r^2(t - t_w, t_w)\rangle$ and the corresponding superposition $[\langle r^2(\xi - \xi_w)\rangle]$ are shown in the ESI† (Fig. S1 and S2). The values of α, needed to obtain the superposition, exhibit an increase with increasing concentration of LAPONITE®, indicating that the relaxation time evolves at a faster rate.

The superpositions obtained for all the three LAPONITE® concentrations are plotted in Fig. 6. The shape of the curve does not exhibit any obvious dependence on the LAPONITE® concentration. Since the MSD has been equated with the creep compliance, the very fact that the shape of superposition is preserved over the three decades of timescales suggests that the shape of the relaxation time spectrum remains unchanged by the change in the LAPONITE® concentration. Interestingly, the observed behavior corroborates quite well with that observed by Shahin and Joshi[35] for bulk rheological measurements, wherein the shape of a spectrum of the relaxation times was observed to remain unchanged with the change in the LAPONITE® concentration. The values of $\langle r^2(\xi - \xi_w)\rangle$ shown in Fig. 6, as expected, are

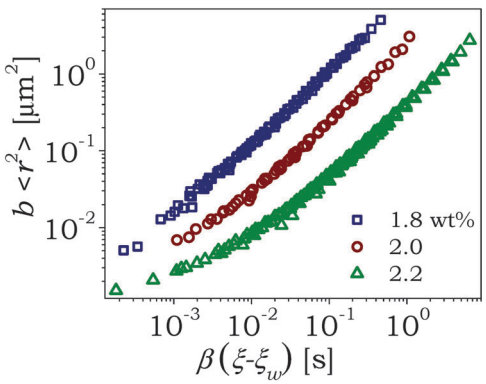

Fig. 6 Variation of superimposed MSD($\langle r^2\rangle$) with the effective time difference ($\xi - \xi_w$) for an aqueous LAPONITE® suspension of different concentrations. The values of α are: 0.04 ± 0.0017 (1.8%), 0.077 ± 0.0013 (2%) and 0.105 ± 0.007 (2.2%). A slight vertical shifting is needed for the 2.2 weight% suspension, whose values are given in the ESI;† for the other two concentrations we do not need any vertical shifting. The factor β carries no physical meaning and is simply used to translate the curves horizontally to show the superimpositions more clearly (β = 0.1 for 1.8%, 0.3 for 2.0% and 1 for 2.2%).

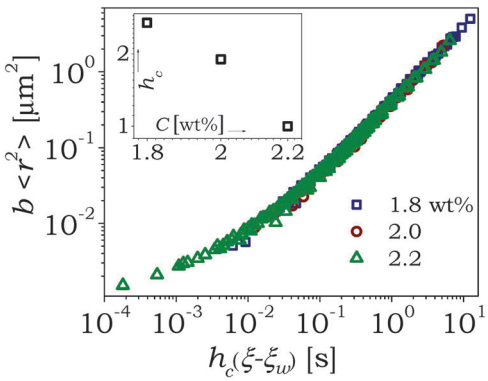

Fig. 7 The global master MSD($\langle r^2\rangle$) curve plotted in the effective time domain, obtained by horizontally shifting the three master curves corresponding to three different LAPONITE® concentrations, shown in Fig. 6. The inset shows the horizontal shift factors ($h_c = \bar{\tau}(c_{L,R})/\bar{\tau}(c_L)$) plotted as a function of the LAPONITE® concentration.

seen to decrease with the increase in the LAPONITE® concentration, suggesting that the mean relaxation time increases with the increase in the LAPONITE® concentration. The values of $\langle r^2(\xi - \xi_w)\rangle$, for LAPONITE® concentrations of 1.8 weight% and 2 weight%, are shifted horizontally to overlay on the data for the reference concentration ($c_{L,R}$ = 2.2 weight%) leading to a master superposition [time–aging time–LAPONITE® concentration superposition] as shown in Fig. 7. The horizontal shift factor given by $h_c = \bar{\tau}(c_{L,R})/\bar{\tau}(c_L)$ is plotted in the inset of Fig. 7. As expected, h_c, which is proportional to the inverse of the relaxation time, decreases with the increase in the LAPONITE® concentration (c_L). A slight vertical shifting is needed only for the 2.2 weight% suspension in order to get better quality of superposition; the corresponding shift factors (b) are shown in Fig. S3 (ESI†).

The ordinate of Fig. 7 that shows master superposition of $\langle r^2(\xi - \xi_w)\rangle$ is also equivalent to $(k_BT/\pi a)J(\xi - \xi_w)$. With the knowledge of creep compliance in the effective time domain, the stress relaxation modulus, then, can be obtained using the convolution relation given by:

$$\xi = \int_0^{\xi} J(\xi - \zeta)G_r(\zeta)\mathrm{d}\zeta \quad \text{or}$$
$$\mathcal{L}\{J(\xi)\}\mathcal{L}\{G_r(\xi)\} = \tilde{J}(p)\tilde{G}_r(p) = 1/p^2 \quad (9)$$

where, p is the Laplace frequency. Eqn (9) is identical to eqn (2) in every aspect except that the real time in the latter is replaced by the effective time in the former $\left[\tilde{f}(p) \equiv \mathcal{L}\{f(\xi)\} \equiv \int_0^{\infty} e^{-p\xi} f(\xi)\mathrm{d}\xi\right]$. We solve eqn (9) numerically by using the scheme proposed by Zhu *et al.*[46] to obtain the relaxation modulus in the effective time domain given by $(\pi a/k_BT)G_r(\xi - \xi_w)$, which is shown in the inset of Fig. 8. Fig. 8 shows the relaxation modulus associated with an individual LAPONITE® concentration, which is obtained by dividing the abscissa in the inset of Fig. 8 by the horizontal shift factor (h_c) plotted in the inset of Fig. 7, which leads to the separation of superpositions associated with each concentration. It can be seen that the predicted relaxation modulus is constant

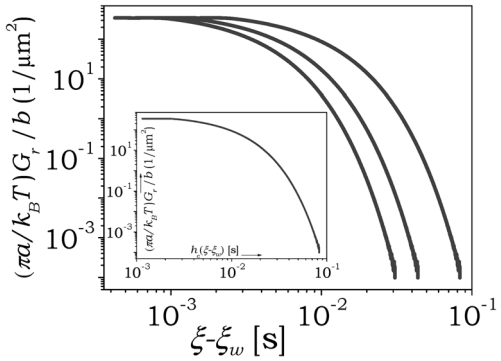

Fig. 8 The individual superposition of stress relaxation modulus ($\pi a/k_BT)G_r(t)$ in the effective time domain for the three studied concentrations: from left to right 1.8, 2 and 2.2 weight%, which are obtained from the master superposition of the stress relaxation modulus plotted in the effective time domain (by using global master MSD curve shown in Fig. 7 by solving eqn (9)), shown in the inset.

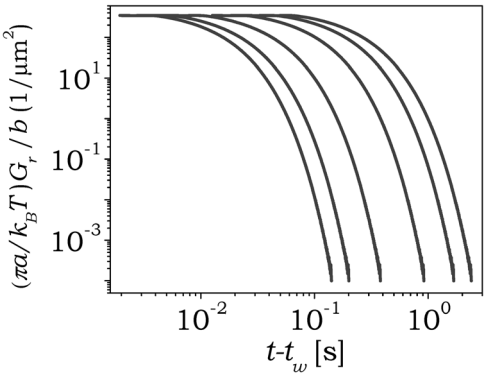

Fig. 9 The time evolution of the stress relaxation modulus ($\pi a/k_BT)G_r(t)$ is plotted in the real time domain for different t_w (from left to right: 15, 20, 30, 40, 45, and 50 min) for a 2 weight% LAPONITE® suspension obtained from eqn (10).

in the limit of very small effective times and decreases with the increase in $\xi - \xi_w$, and eventually decays to zero. As expected, the relaxation gets delayed in time with the increase in the LAPONITE® concentration.

The global master superposition for $\langle r^2(\xi - \xi_w)\rangle$ or $(k_BT/\pi a)J(\xi - \xi_w)$ shown in Fig. 7 and that of $(\pi a/k_BT)G_r(\xi - \xi_w)$ shown in Fig. 8 describe the behavior of respective parameters if the experiments were conducted for a system having concentration $c_{L,R}$ in the effective time domain. The creep compliance (or MSD) and stress relaxation data in the effective time domain can be transformed back to the real time domain by simply inverting eqn (8) to give:

$$t - t_w = \ln[(e^{-\alpha t_w} - \alpha\{\xi - \xi_w\})^{-1/\alpha}] - t_w. \qquad (10)$$

The master superposition of the MSD data shown in Fig. 6 is therefore inverted to predict the MSD behavior of the 2 weight% LAPONITE® system as shown by solid lines in Fig. 2. An interesting point to note is that the prediction is obtained over the five time decades, while the original data available are for a span of over only two decades. Moreover, the procedure does not simply predict the MSD behavior over greater magnitudes of lag time, but also for very small values of lag time, much below the time resolution achieved using the CCD camera employed for acquiring the images. Such enhanced prediction in both the time limits is enabled by the definition of effective time, wherein the real time is normalized by the relaxation time. Consequently, the smaller relaxation time contributions (low concentrations of LAPONITE® and/or small t_w) to the superposition facilitate the prediction of the MSD over greater lag times, while those of large relaxation times (large concentrations of LAPONITE® and/or large t_w) allow predictions of very short lag times. Furthermore, the original experimental data are available only in a limit of very small lag times compared to the aging time ($t - t_w \ll t_w$). However, the prediction is obtained for significantly higher lag times, which indeed accounts for the aging that occurs during a course of lag time. Fig. 2 also demonstrates the MSD plateau in a limit of large time scales, which is due to overall jamming in a material typically observed when relaxation time scales are larger than linear.[10] Lastly, we also obtain the stress relaxation behavior in the real time domain, as shown in Fig. 9 for a 2 weight% LAPONITE® concentration. The stress relaxation gets slower with the increase in t_w and the very fact that the stress relaxes completely suggests that the LAPONITE® suspension is in the sol state over the duration explored in the present work.

Knowledge of $G_r(t)$ at various t_w also allows us to obtain complex modulus G^*, as a function of ω by using:

$$G^*(\omega) = G' + iG'' = i\omega\int_0^\infty G_r(t)e^{-i\omega t}dt. \qquad (11)$$

Even though the material is time dependent, as the relaxation modulus decays over a period much smaller than t_w as shown in Fig. 9, eqn (11) can be used to obtain G^*. We plot G' and G'' obtained from eqn (11) for $\omega = 10$ rad s^{-1} as a function of t_w in Fig. 1(a) and as a function of ω for $t_w = 1800$ s in Fig. 1(b). Both figures clearly show that G' and G'' predicted from the microrheology experiments are significantly lower than that of the experimental data. Moreover, it can be seen from Fig. 1(a) that the time at which G' and G'' cross each other is much smaller for the bulk rheology data ($\approx$900 s) compared to the microrheology data ($\approx$3000 s), although the value of modulus associated with the crossover is comparable. We believe that both these observations are due to the fractal nature of a growing LAPONITE® gel. After thoroughly mixing LAPONITE® powder in water, the particles of LAPONITE® start aggregating under quiescent conditions. The aggregates having different sizes grow with time, and consequently the void space that contains primarily water and stray LAPONITE® particles keeps shrinking. It is interesting to note that while the growing aggregates may interact with each other over the macroscopic length-scales, the pockets in between the aggregates with length-scale greater than that of tracer particles still contain the viscous liquid. In the initial stages of the experiment the material is primarily viscous over the microscopic scale, while the structure builds up on the macroscopic scale, which results in the magnitude of G' and G'' obtained from the bulk measurements to be greater

than that obtained from the microrheology experiments. However, as the viscous pockets shrink, the tracer particles get confined to progressively smaller spaces leading to G' and G'' crossing each other at longer times. Interestingly, the values of the modulus at the crossover for both bulk rheology and microrheology, however, match each other. Similar observations showing differences between the bulk rheology and microrheology measurements have been reported previously.[24,33] It should, however, be noted that while the bulk and microrheology data for the LAPONITE® suspension do not match due to heterogeneities, the microrheology data show an excellent match with the bulk rheological data for many soft materials that are homogeneous over the probe particle length-scale.[47–49]

The present work clearly demonstrates several advantages of carrying out analysis of time dependent soft materials in the effective time domain. The extra time dependence incorporated in eqn (5) states that the values of MSD get affected by aging that occurs during the lag time, when the lag time is of the order of aging time $[t - t_w = O(t_w)]$ and consequently, eqn (1)–(3) cannot be applied to such time dependent materials. While such restriction affects all the aging times, it critically affects the measurements at the beginning of aging (small t_w). However, once MSD experiments have been performed in the limit of smaller lag times ($t - t_w \ll t_w$), whence the eqn (1)–(3) are applicable, expressing the MSD data obtained at different t_w in the effective time domain allows a linear viscoelastic representation of the same, which otherwise is not possible. Moreover, since the relaxation time is small at low t_w, it facilitates the prediction of long time MSD behavior (and in general, the rheological behavior) over large lag times. Equivalently, the MSD data at large t_w facilitates prediction over very small lag times. The present work even goes one step further wherein superposition has also been obtained by accommodating LAPONITE® concentration dependence. Such superpositions, which have been proposed to be valid for bulk rheological measurements, allow the prediction of the MSD over much greater lag times.[35] The major requirement for the feasibility of such analysis is a prior knowledge of relaxation time dependence on time, which can be obtained either independently or through the process of obtaining superposition itself. It is also important to note that the applicability of effective time domain expressed by eqn (6) is not only limited to a single relaxation time dependence, but also to various functional forms of $\tau(t)$ at different times that can be easily accommodated in eqn (6) as a sum of the integrals.

IV. Conclusion

In the present work, the rheological behavior of time dependent (physically aging) aqueous suspensions of LAPONITE®, a model soft glassy material, is studied using a passive microrheology technique. We employ an optical microscope to probe the thermal motion of micron-sized tracer particles embedded in the sample. The motion of the tracer particles shows purely diffusive behavior at short aging times that progressively changes to subdiffusive behavior as the material ages. We obtain the MSDs for different aging times (t_w) and for suspensions of three different LAPONITE® concentrations in such a way that the lag time ($t - t_w$) is very small ($t - t_w \ll t_w$). Within the range of lag times studied, the variation of relaxation time is negligible, and so the MSD can be equated to the creep compliance using standard microrheology analysis. The MSDs obtained at different aging times as well as LAPONITE® concentrations, however, possess different relaxation times. In order to get rid of time dependency, we employ a concept of effective time, wherein the real time is normalized by the time dependent relaxation time to readjust the material clock. Consequently, we transform the MSD data from the real time domain to the effective time domain that results in time–aging time superposition. Interestingly, the time–aging time superpositions for different LAPONITE® concentrations show similar shapes, which eventually leads to a time–aging-time–concentration master curve. The existence of such a master curve, which has also been previously observed, but for the macroscopic rheological behavior of LAPONITE® suspensions, suggests that the aging time as well as the LAPONITE® concentration only affects the mean relaxation time but not the shape of the relaxation time distribution. Since the MSD behavior of tracer particles is qualitatively analogous to the creep compliance, the use of the standard convolution relation of linear viscoelasticity in the effective time domain allows the prediction of the stress relaxation behavior of the suspension. Interestingly the transformation of both creep compliance (MSD) and stress relaxation data from the effective time domain to the real time domain leads to the real time behaviors of the respective parameters at different aging times and LAPONITE® concentrations. Particularly, for the MSD, such transformation allows prediction over larger lag times (over five decades) compared to those incorporated in experimental measurements (around two decades), demonstrating the significant advantage of the proposed approach. Overall, we believe that the effective time domain approach provides an important step forward in analyzing time dependent materials using microrheological techniques.

Acknowledgements

The financial support from the Department of Atomic Energy – Science Research Council, Government of India, is greatly acknowledged.

References

1 Y. M. Joshi, *Annu. Rev. Chem. Biomol. Eng.*, 2014, **5**, 181–202.
2 P. Cicuta and A. M. Donald, *Soft Matter*, 2007, **3**, 1449–1455.
3 T. M. Squires and T. G. Mason, *Annu. Rev. Fluid Mech.*, 2010, **42**, 413–438.
4 A. M. Puertas and T. Voigtmann, *J. Phys.: Condens. Matter*, 2014, **26**, 243101.
5 K. M. Schultz and E. M. Furst, *Soft Matter*, 2012, **8**, 6198–6205.
6 A. A. Abdala, S. Amin, J. H. van Zanten and S. A. Khan, *Langmuir*, 2015, **31**, 3944–3951.

7 T. Moschakis, *Curr. Opin. Colloid Interface Sci.*, 2013, **18**, 311–323.
8 M. E. Cates and M. R. Evans, *Soft and fragile matter*, The Institute of Physics Publishing, London, 2000.
9 S. M. Fielding, P. Sollich and M. E. Cates, *J. Rheol.*, 2000, **44**, 323–369.
10 A. Shahin and Y. M. Joshi, *Phys. Rev. Lett.*, 2011, **106**, 038302.
11 M. Kaushal and Y. M. Joshi, *Soft Matter*, 2014, **10**, 1891–1894.
12 M. Kaushal and Y. M. Joshi, *Macromolecules*, 2014, **47**, 8041–8047.
13 G. B. McKenna, T. Narita and F. Lequeux, *J. Rheol.*, 2009, **53**, 489–516.
14 T. G. Mason and D. A. Weitz, *Phys. Rev. Lett.*, 1995, **74**, 1250–1253.
15 T. A. Waigh, *Rep. Prog. Phys.*, 2005, **68**, 685–742.
16 T. A. Waigh, *Rep. Prog. Phys.*, 2005, **68**, 685–742.
17 J. Liu, M. L. Gardel, K. Kroy, E. Frey, B. D. Hoffman, J. C. Crocker, A. R. Bausch and D. A. Weitz, *Phys. Rev. Lett.*, 2006, **96**, 118104.
18 J. C. Crocker and D. G. Grier, *J. Colloid Interface Sci.*, 1996, **179**, 298–310.
19 X. Jingyuan, V. Virgile and D. Wirtz, *Rheol. Acta*, 1998, **37**, 387–398.
20 T. G. Mason, *Rheol. Acta*, 2000, **39**, 371–378.
21 J. D. Ferry, *Viscoelastic Properties of Polymers*, 1980.
22 M. T. Valentine, P. D. Kaplan, D. Thota, J. C. Crocker, T. Gisler, R. K. Prud'homme, M. Beck and D. A. Weitz, *Phys. Rev. E: Stat., Nonlinear, Soft Matter Phys.*, 2001, **64**, 061506.
23 D. Weihs, M. A. Teitell and T. G. Mason, *Microfluid. Nanofluid.*, 2007, **3**, 227–237.
24 F. K. Oppong, P. Coussot and J. R. de Bruyn, *Phys. Rev. E: Stat., Nonlinear, Soft Matter Phys.*, 2008, **78**, 021405.
25 M. Caggioni, P. T. Spicer, D. L. Blair, S. E. Lindberg and D. A. Weitz, *J. Rheol.*, 2007, **51**, 851–865.
26 T. Savin and P. S. Doyle, *Soft Matter*, 2007, **3**, 1194–1202.
27 H. A. Houghton, I. A. Hasnain and A. M. Donald, *Eur. Phys. J. E: Soft Matter Biol. Phys.*, 2008, **25**, 119–127.
28 T. H. Larsen and E. M. Furst, *Phys. Rev. Lett.*, 2008, **100**, 146001.
29 F. Chambon and H. H. Winter, *J. Rheol.*, 1987, **31**, 683–697.
30 B. Abou and F. Gallet, *Phys. Rev. Lett.*, 2004, **93**, 160603.
31 S. Jabbari-Farouji, D. Mizuno, M. Atakhorrami, F. C. MacKintosh, C. F. Schmidt, E. Eiser, G. H. Wegdam and D. Bonn, *Phys. Rev. Lett.*, 2007, **98**, 108302.
32 F. K. Oppong, L. Rubatat, B. J. Frisken, A. E. Bailey and J. R. de Bruyn, *Phys. Rev. E: Stat., Nonlinear, Soft Matter Phys.*, 2006, **73**, 041405.
33 J. P. Rich, G. H. McKinley and P. S. Doyle, *J. Rheol.*, 2011, **55**, 273–299.
34 B. Ruzicka and E. Zaccarelli, *Soft Matter*, 2011, **7**, 1268–1286.
35 A. Shahin and Y. M. Joshi, *Langmuir*, 2012, **28**, 15674–15686.
36 J. P. Rich, J. Lammerding, G. H. McKinley and P. S. Doyle, *Soft Matter*, 2011, **7**, 9933–9943.
37 A. Shahin and Y. M. Joshi, *Langmuir*, 2012, **28**, 5826–5833.
38 M. Cloitre, R. Borrega and L. Leibler, *Phys. Rev. Lett.*, 2000, **85**, 4819–4822.
39 A. S. Negi and C. O. Osuji, *Phys. Rev. E: Stat., Nonlinear, Soft Matter Phys.*, 2009, **80**, 010404.
40 P. Coussot, H. Tabuteau, X. Chateau, L. Tocquer and G. Ovarlez, *J. Rheol.*, 2006, **50**, 975–994.
41 R. Gupta, B. Baldewa and Y. M. Joshi, *Soft Matter*, 2012, **8**, 4171–4176.
42 I. L. Hopkins, *J. Polym. Sci.*, 1958, **28**, 631–633.
43 L. C. E. Struik, *Physical Aging in Amorphous Polymers and Other Materials*, Elsevier, Houston, 1978.
44 F. Schosseler, S. Kaloun, M. Skouri and J. P. Munch, *Phys. Rev. E: Stat., Nonlinear, Soft Matter Phys.*, 2006, **73**, 021401.
45 A. S. Negi and C. O. Osuji, *Phys. Rev. E: Stat., Nonlinear, Soft Matter Phys.*, 2010, **82**, 031404.
46 Y. Zhu, L. Sun and H. Xu, *J. Appl. Mech., Trans. ASME*, 2011, **78**, 031002.
47 M. Tassieri, F. D. Giudice, E. J. Robertson, N. Jain, B. Fries, R. Wilson, A. Glidle, F. Greco, P. A. Netti, P. L. Maffettone, T. Bicanic and J. M. Cooper, *Sci. Rep.*, 2015, **5**, 8831.
48 M. Buchanan, M. Atakhorrami, J. F. Palierne, F. C. MacKintosh and C. F. Schmidt, *Phys. Rev. E: Stat., Nonlinear, Soft Matter Phys.*, 2005, **72**, 011504.
49 G. Pesce, A. C. D. Luca, G. Rusciano, P. A. Netti, S. Fusco and A. Sasso, *J. Opt. A: Pure Appl. Opt.*, 2009, **11**, 034016.